A new modelling for Damage Initiation and Propagation of Randomly-Oriented Thermoplastic Composites

Kei Saito[1], Seiji Hayashi[2], Mitsuharu Kan[2], Masato Nishi[1]

[1]JSOL Corporation, 2-5-24 Harumi, Chuo-ku, Tokyo, Japan
[2]Honda R&D Co., Ltd., 4630, Shimotakanezawa, Haga-Machi, Haga-gun, Tochigi, Japan

1 Abstract

A new method to model damage properties of Randomly-Oriented Thermoplastic Composites (RO-FRTP) was proposed for finite element analysis (FEA). The materials are composites of thin sheets in which carbon fibers of approximately one inch in length are distributed randomly in thermoplastics resin matrix. While their material properties are intrinsically isotropic in plane from a macro perspective, RO-FRTP have complex nature of damage initiation and progression that depends on the deformation mode. In this study, the damage model that based on Continuum Damage Mechanics (CDM) was developed and the modelling method with 3D shell element for RO-FRTP was proposed. The multifunctional feature of ***MAT_ADD_GENERALIZED_DAMAGE** in LS-DYNA® has been utilized in order to reproduce damage properties of the material. Furthermore, several numerical studies are conducted and compared to experiments for the purpose of validation of the modelling method. Simulation results show that the modelling method can capture complex damage characteristics of the material in detail and predict deformation of structures accurately.

2 Introduction

Recently thermosetting continuous Carbon Fiber Reinforced Plastics (CFRP) have applied especially in high-end vehicles for weight reduction in order to enhance automobile maneuverability and fuel efficiency. Unidirectional (UD) composites have also been used in body structures of vehicle because of its lower material unit cost compared to cross composites. Although manufacturing technologies for mass production for UD composites have been established and utilized, the cost is still higher than conventional materials such as steels and aluminum alloys and it prevents the material from further use in vehicle structures. RO-FRTP is one of the candidates that can improve the production cost and the efficiency. Generally, components made of RO-FRTP are manufactured by press forming of heated pre-consolidated sheets for which it takes about one minute to be processed. In addition, the material unit cost is lower than that of CFRP as well. Actually, the material has been investigated and applied to automotive parts in some vehicles [1]. On the other hand, there is little study about modelling methods for Computer Aided Engineering (CAE), which is essential for the efficient design process.

Thin sheet of RO-FRTP consists of matrix resin and chopped fibers that are randomly distributed in the material. Schematic image of a RO-FRTP sheet is represented in Fig.1. While the in-plane material property is isotropic, characteristics in tension and compression are different. Furthermore, the out-of-plane transverse shear modulus is different from the in-plane shear modulus due to the contribution of fibers to the transverse stiffness. Damage properties of the material are also characteristic. The in-plane damage initiation and progression depend on the deformation mode. The out-of-plane damage is also remarkable and the damage accumulation is affected by the in-plane damage. In order to model the in-plane material characteristics, elastic plastic material models that can express different properties between tension and compression are generally preferred. However, it may be challenging for these kind of material models to reproduce the deformation mode of RO-FRTP in which transverse deformation can be dominant like three-point bending tests. Fig.2 (a) shows stress-strain curves in tension and compression that are prepared for the conventional material model, ***MAT_124** in LS-DYNA®. Fig.2 (b) shows comparison of reaction force between the experiment and the simulation with the material model. While the reaction force of the simulation increases in a linear manner, the force measured in the experiment shows the non-linear property up to the peak point. This non-linearity is caused by the damage of the out-of-plane shear modulus. It has been reported that considering the out-of-plane damage is necessary to obtain the same trend observed in the

experiment [2]. For efficient design process with CAE, a modelling method that can predict the damage initiation and progression of RO-FRTP with a high degree of accuracy is required.
In this study, the material and damage modelling for RO-FRTP is proposed. Considering the thickness of RO-FRTP sheets and computation costs for the practical use of the analysis, the modelling method is mainly developed for 3D shell element. The multifunctional damage modelling tool, ***MAT_ADD_GENERALIZED_DAMAGE** (**MAGD**) which has been recently introduced in LS-DYNA® [3][4], is applied to the damage modelling. The feature provides several modelling options not only for the isotropic but also for the anisotropic damage progression with multiple damage parameters accumulated in the way based on Generalized Incremental Stress State Dependent Damage Model (GISSMO) [5]. The damage model defines and accumulates damages in stress triaxility space. Therefore, different damage progression that depends on the deformation mode can be achieved with a single model. GISSMO usually accumulates damages according to equivalent plastic strain, but **MAGD** can also accept and use the other variables passed from material models as damage associated parameters. Since the feature is generalized for a flexible use of modelling damage, it can be applied to RO-FRTP which have complex nature of damage progression. For a validation of the modelling method, several numerical simulations were conducted and were compared to experimental results. Simulation results show that the modelling method can capture the damage progression in detail and predict the deformation of RO-FRTP products accurately.

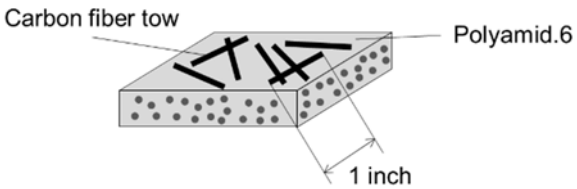

Fig.1: Schematic image of RO-FRTP sheet.

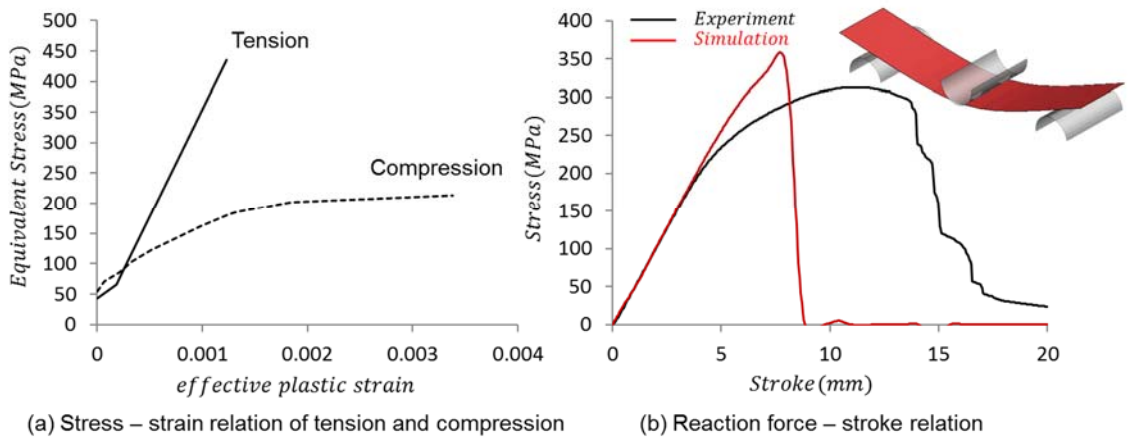

(a) Stress – strain relation of tension and compression (b) Reaction force – stroke relation

Fig.2: Simulation of the three-point bending test of flat plate: (a) stress – strain curves in different deformation modes, (b) comparison of reaction force from the test and CAE with the conventional material model.

3 Material and damage characteristics of RO-FRTP

The material consists of chopped carbon fiber tows of approximately one inch in length and Polyamide.6 as the matrix resin. The material composition is shown in Table 1. In this study, a modelling of RO-FRTP sheets of approximately 1.6mm in thickness was investigated. Since fibers are distributed and aligned randomly in the sheet, the material exhibits in-plane isotropy. On the other hand, fibers do not align in thickness direction as shown in Fig.1. Therefore, the transverse shear modulus is different from the in-plane shear modulus. Basic mechanical properties are shown in Table 2. The tensile property was obtained in conformance with JIS K7164 [6], the compression property in conformance with JIS K7076 [7], and the flat plate three-point bending property in conformance with JIS K7074 [8]. In order to identify material and damage properties of RO-FRTP sheets with the aim of

simulating three-point bending tests, extensive experiments have been carried out and studied in detail [10]. In this section, several properties that are important for the numerical simulation are briefly mentioned from the reference.

Carbon fiber	Figure	Chopped tow
	Length	1 inch
	Volume Fraction	35%
Matrix	Polymer	Polyamid.6

Table 1: Material composition

Young's modulus		23.3GPa
Poisson's ratio		0.32
Strength	Tension	435MPa
	Compression	238MPa
	Bending	378MPa

Table 2: Basic mechanical properties

3.1 In-plane damage properties

Damage progressions under tensile, compressive, and shear loading mode are shown in Fig.3. The horizontal axis represents the measured strain in each mode and the vertical axis the damage value (unity means complete loss of area transmitting loads). In the tensile deformation, the material has the aspect of brittle fracture which causes a sudden load drop in the three-point bending test. The compressive damage progression is obtained by the compression continuous stress test which can accurately capture the same damage progression that is observed in three-point bending tests [10]. In the compressive deformation, the damage develops non-linearly after the damage initiation. Fig.4 (a) shows compressive stress and strain measured in the experiment. After reaching the strength, the stress keeps nearly constant, accumulating the damage during successive deformation. These properties under the compressive loading cause the characteristic stress redistribution in thickness direction during the bending deformation and contribute to the ductile behavior seen in the three-point bending test. The damage progression under the shear mode is obtained by a JIS K7079 [9]. In the shear deformation, the damage develops non-linearly as well. However, the trend of damage progression is different from the other deformation mode. Fig.4 (b) shows the shear stress and strain measured in the experiment.
These experiments reveal that damage properties of RO-FRTP strongly depend on the loading mode. This means that the damage initiation and propagation can be described as a function of stress triaxiality, which is a parameter that expresses stress states in a plane stress condition.

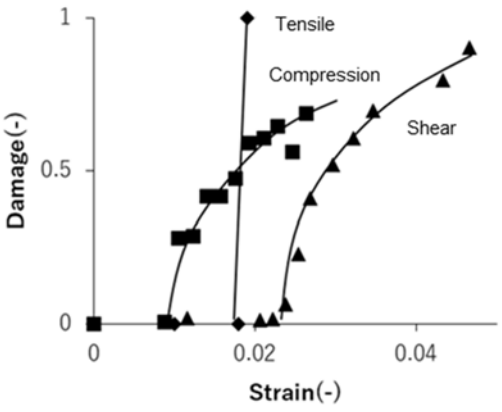

Fig.3: Damage progression curve in each loading condition

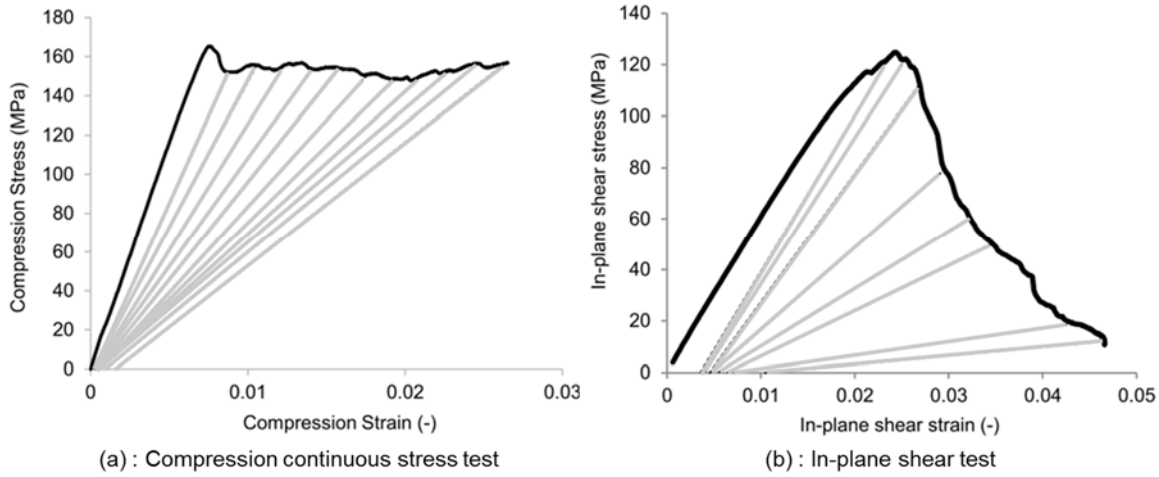

Fig.4: Results of compression continuous stress test and the in-plane shear test.

3.2 Out-of-plane shear damage properties

The out-of-plane shear property of RO-FRTP was obtained by the double-notched specimen for the out-of-plane shear test with cyclic loadings that are proposed by Matsuo et al. [11]. Compared to conventional tests with double-notched specimen, the proposed test can yield wider area of shear deformation and provide direct strain measurements with a strain gage. Fig. 5 (a) shows the out-of-plane stress-strain curve obtained by the experiment. The property of the out-of-plane shear deformation is different from the in-plane deformation because fibers are not aligned in thickness direction. Fig.5 (b) shows the damage progression according to the out-of-plane shear strain obtained by the measurement of stiffness change during cyclic loadings. There is also remarkable damage progression in this deformation mode. Since the stiffness in the out-of-plane direction is relatively smaller than the in-plane elastic stiffness property, it contributes greatly to the ductile behavior that was observed in the three-point bending test. It was also found that the out-of-plane shear damage is affected by the previously accumulated in-plane damage. The relation between the in-plane compressive damage and the out-of-plane damage was obtained by the three-point bending test of flat plate that has compressive damage in advance [10].

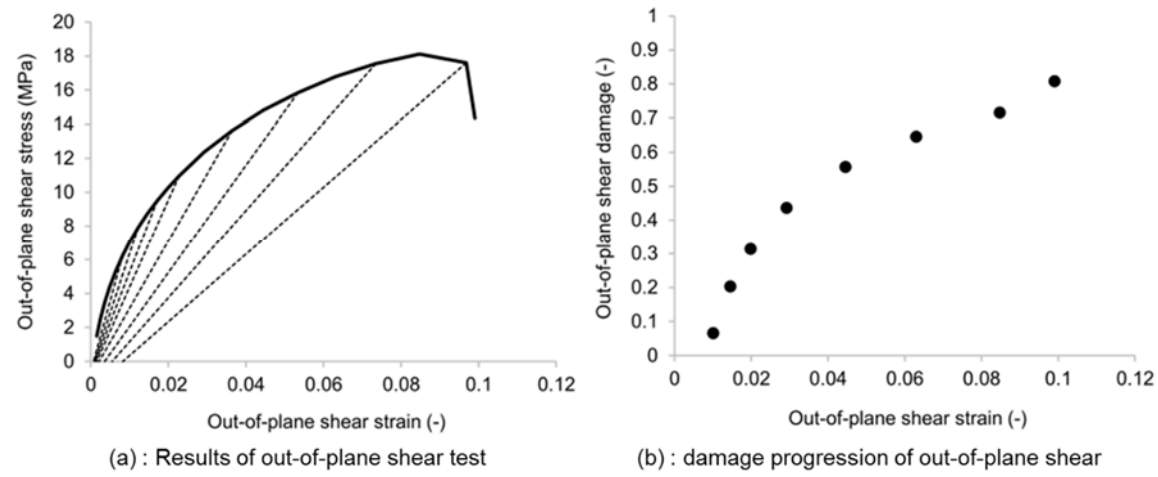

Fig.5: The damage property of the out-of-plane shear deformation.

3.3 Strain rate dependence

RO-FRTP has a strain rate dependence due to the property of resin materials. As previously mentioned, material properties of RO-FRTP depend on the loading mode. In order to obtain the macroscopic effect of rate dependency, the dynamic three-point bending test that includes all the

deformation modes was conducted and examined. From the bending strength measured in a set of experiments, Cowper-Symonds coefficients were determined to interpolate the rate dependency [10].

4 Damage model

As explained in the previous section, RO-FRTP exhibits remarkable damage properties in both the in-plane and the out-of-plane deformation in the process leading to fracture. Furthermore, the in-plane damage initiation and progression of RO-FRTP depend on stress states during the deformation. In this study, we developed a new damage model which is based on CDM in order to consider the characteristic damage of RO-FRTP.

4.1 Material constitutive law

The constitutive law of RO-FRTP is modeled as isotropic elastic material and described in Voigt notion as

$$\begin{Bmatrix}\sigma_{11}\\ \sigma_{22}\\ \tau_{12}\end{Bmatrix} = (1-d^{in})\begin{bmatrix}2G_{12}+\lambda & \lambda & 0\\ \lambda & 2G_{12}+\lambda & 0\\ 0 & 0 & G_{12}\end{bmatrix}\begin{Bmatrix}\varepsilon_{11}\\ \varepsilon_{22}\\ \gamma_{12}\end{Bmatrix} \quad (1)$$

where σ_{11}, σ_{22}, and τ_{12} are the in-plane true stress, ε_{11}, ε_{22}, and γ_{12} are the in-plane true strain, G_{12} is the in-plane shear modulus and λ is Lame constant which is expressed as $\lambda = \nu E/(1+\nu)(1-2\nu)$ where E is Young's modulus and ν is Poisson's ratio. The isotropic damage progression is assumed and expressed by a single parameter d^{in}. Constitutive equation of the out-of-plane shear is described as

$$\tau_{23} = G_{23}(1-d^{ts})\gamma_{23} \quad (2)$$

$$\tau_{31} = G_{31}(1-d^{ts})\gamma_{31} \quad (3)$$

where τ_{ij} is the out-of-plane true stress, γ_{ij} is the out-of-plane true strain and G_{23} and G_{31} are the out-of-plane shear modulus. The out-of-plane damage is expressed by a single parameter d^{ts}.

4.2 In-plane damage progress law

In order to reproduce the in-plane damage property of RO-FRTP, the damage progress law was applied, which is defined as a function of stress triaxiality and use thermodynamic force as the damage driving parameter. The damage law can describe the damage initiation and evolution of each deformation mode continuously in the same space. The in-plane elastic potential energy of the material is expressed by the following equation.

$$\psi^{in} = \frac{\sigma_1^2}{2E(1-d^{in})} + \frac{\sigma_2^2}{2E(1-d^{in})} - \frac{\nu}{E}\frac{\sigma_1\sigma_2}{(1-d^{in})} \quad (4)$$

where σ_i is the in-plane principal stress component. The in-plane thermodynamic force Y^{in} can be derived as following eqution from eq. (4)

$$Y^{in} = -\frac{\partial\psi^{in}}{\partial d^{in}} = \frac{\sigma_1^2}{2E(1-d^{in})^2} + \frac{\sigma_2^2}{2E(1-d^{in})^2} - \frac{\nu}{E}\frac{\sigma_1\sigma_2}{(1-d^{in})^2} \quad (5)$$

Andrade et al. [5] have proposed GISSMO which is the accumulation type damage progress model that uses stress triaxiality to model the stress state dependency and equivalent plastic strain as the damage driving parameter. In this study, thermodynamic paremter Y^{in} is used instead of euqivalent plastic strain. In this case, the rate of damage paremter $\dot{D}$ is expressed as

$$\dot{D}(Y^{in}) = \frac{\beta D^{1-\frac{1}{\beta}}}{\sqrt{Y_f^{in}(\eta,\dot{\bar{\varepsilon}})}}\sqrt{\dot{Y}_{max}^{in}} \quad (6)$$

where β is an exponent that controls the damage progress and Y_{max}^{in} is the maximum value of Y^{in} experienced before. In addition, $Y_f^{in}(\eta,\dot{\bar{\varepsilon}})$ is the thermodynamic force at the fracture which is defined as a function of strain rate $\dot{\bar{\varepsilon}}$ and stress triaxiality defined as

$$\eta = \frac{\sigma_m}{\bar{\sigma}} \quad (7)$$

where σ_m is mean stress and $\bar{\sigma}$ is equivalent stress. The damage parameter is integrated according to (6) and the material is asumed to be completely fractured when D reaches unity. That is to say, when the strain rate and the stress state are ideally kept constant ($\dot{\bar{\varepsilon}} = s, \eta = t$), fracture is occured when $Y^{in} = Y_f^{in}(s,t)$. In order to model the stress degradation due to the damage, the method which based on CDM is applied to the damage modelling. The relation between true stress and effective stress is simply expressed by a single damage parameter d^{in} as

$$\sigma_{ij} = (1 - d^{in})\tilde{\sigma}_{ij} \tag{8}$$

where $\tilde{\sigma}_{ij}$ is effective stress component in the in-plane direction. By the method similar to equation (6), the following parameter F is introduced as the criterion for the beggining of the influence of damage on the constitutive law [5]

$$\dot{F}(Y^{in}) = \frac{F}{\sqrt{Y_{crit}^{in}(\eta, \dot{\bar{\varepsilon}})}} \sqrt{\dot{Y}_{max}^{in}} \tag{9}$$

where $Y_{crit}^{in}(\eta, \dot{\bar{\varepsilon}})$ is Y^{in} when a coupling of the constitutive law of equation (1) and the damage starts, and it is the function of stress triaxiality and strain rate. The parameter d^{in} which is coupled to the constitutive law is expressed as the following equation

$$d_{in} = \begin{cases} 0 & , \ F < 0 \\ \left(\frac{D - D_{crit}}{1 - D_{crit}}\right)^m & , \ F = 1 \end{cases} \tag{10}$$

where m is the exponential parameter controling the coupling to the constitutive law and D_{crit} is the damgage parameter when F reaches unity.

4.3 Out-of-plane damage progress law

The damage of RO-FRTP related to the out-of-plane shear component is expressed as a function of the out-of-plane shear strain

$$d^{ts} = d^{ts}(\bar{\gamma}) \tag{11}$$

where $\bar{\gamma}$ is the equivalent shear strain defined as a square root of a summation of the out-of-plane strain component γ_{23} and γ_{31}

$$\bar{\gamma} = \sqrt{\gamma_{23} + \gamma_{31}} \tag{12}$$

The out-of-plane true stress component τ_{ij} is calculated by a single damage parameter d^{ts} as

$$\tau_{ij} = (1 - d^{ts})\tilde{\tau}_{ij} \tag{13}$$

where $\tilde{\tau}_{ij}$ is the out-of-plane effective stress component. As mentioned in the previous section, the out-of-plane damage of RO-FRTP can be affected by the in-plane damage of which the material experienced before. In order to consider the coupling of the in-plane and the out-of-plane damage, the out-of-plane damage is expressed as below.

$$d^{ts} = \max\left(d^{ts}(\bar{\gamma}), d^{ts'}\left(d_{comp}^{in}\right)\right) \tag{14}$$

where $d^{ts'}\left(d_{comp}^{in}\right)$ is the out-of-plane damage induced by the in-plane compressive damage which is identified by the pre-damaged experiment mentioned in the previous section.

5 Damage modelling with MAGD

The damage modelling for RO-FRTP is achieved by **MAGD** which is the highly functional damage modelling tool equiped in LS-DYNA®. As metioned in the previous section, the damage initiation and progression are described by two pairs of function that are defined in stress triaxiality space and the damage is accumulated with GISSMO algorithm. Fig.6 shows a schematic image of the damage modelling with the method. In the graph, vertical axis represents square root of thermodynamic force and abscissa axis represents stress triaxiality. The two damage driving fuctions are modeled as a piecewise linear curve define by the keyword ***DEFINE_CURVE** and input as the parameter LCSDG and ECRIT in the keyword deck of **MAGD**.

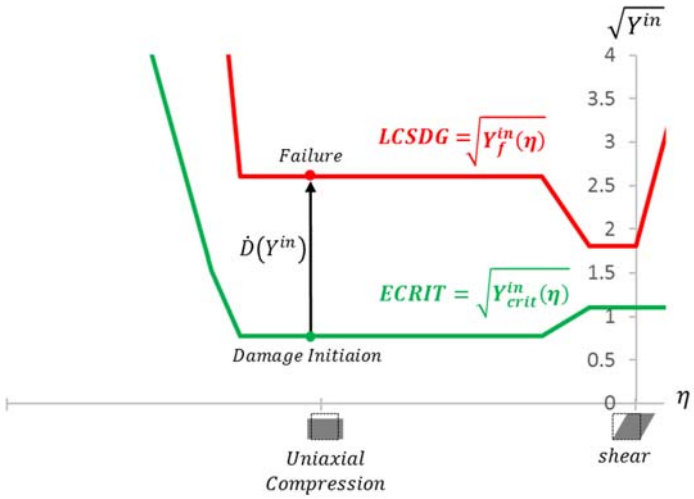

Fig.6: Schematic image of damage modelling by GISSMO algorithm.

The damage modelling feature **MAGD** accepts material history variables as damage driving parameters. In order to model the current damage algorithm with **MAGD**, a material model that can transfer parameters that are necessary for the model is mandatory. The damage modelling also requires the material model to consider elastic plastic deformation and to calculate the in-plane stress and out-of-plane shear stress component independently, so that the characteristic out-of-plane deformation is modelled appropriately. The rate dependent modelling with Cowper-Symonds method is also required. However, there is no such model in a set of standard material models implemented in LS-DYNA®. Therefore, the material model designed for the damage modelling has been developed and implemented in the user material subroutine of LS-DYNA®. Fig.7 shows input and output variables of the user defined material model and **MAGD**, and how the calculation is processed to model the damage effect. For the in-plane damage, the material subroutine calculates effective stress component from the incremental strain. It also calculates thermodynamic force from the effective stress component and stores it as a material history variable. In **MAGD**, the single in-plane damage parameter is accumulated in accordance with GISSMO, referring to the user defined damage property. For the out-of-plane damage, the material subroutine calculates the out-of-plane effective stress component independently from the incremental strain. The out-of-plane damage driving parameter, and the effective strain of transverse direction, are calculated as well. While the in-plane incremental damage depends on stress triaxiality, the out-of-plane damage is accumlated regardless of stress states. Since the damage does not need GISSMO algorithm, it is determined from the user defined damage evolution property in the material subroutine and simply passed to the successive process. Finally, true stress comonent is calculated from the effective stress compoment as well as the two damage parameters in **MAGD**. True stress compoment is expressed as following Voigt notation

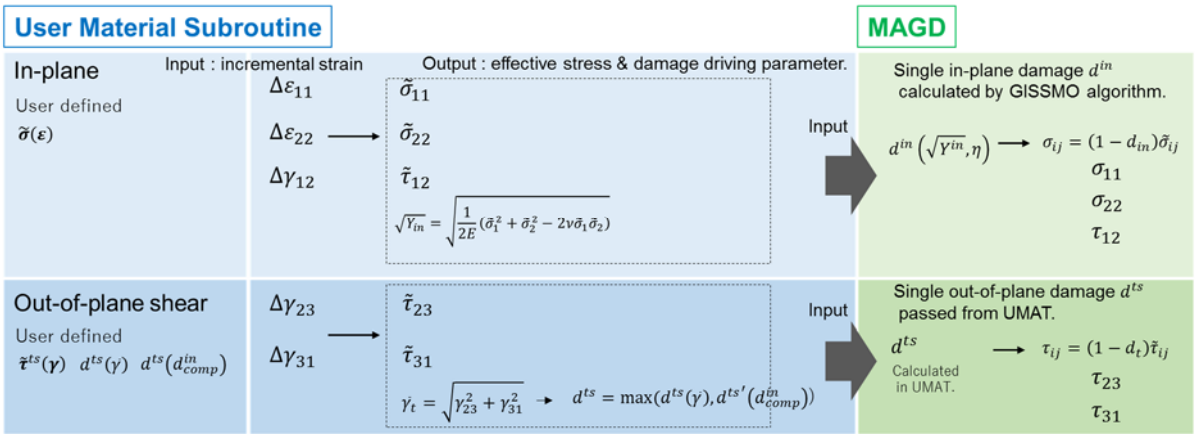

Fig.7: Calculation procedure for true stress component coupled with the in-plane and out-of-plane damage with MAGD.

$$\begin{Bmatrix}\sigma_{11}\\ \sigma_{22}\\ \tau_{12}\\ \tau_{23}\\ \tau_{31}\end{Bmatrix} = \begin{bmatrix}D_{11} & 0 & 0 & 0 & 0\\ 0 & D_{22} & 0 & 0 & 0\\ 0 & 0 & D_{44} & 0 & 0\\ 0 & 0 & 0 & D_{55} & 0\\ 0 & 0 & 0 & 0 & D_{66}\end{bmatrix}\begin{Bmatrix}\tilde{\sigma}_{11}\\ \tilde{\sigma}_{22}\\ \tilde{\tau}_{12}\\ \tilde{\tau}_{23}\\ \tilde{\tau}_{31}\end{Bmatrix} \quad (15)$$

where $D_{11} = D_{22} = D_{44} = 1 - d^{in}$ and $D_{55} = D_{66} = 1 - d^{ts}$ which are defined by the keyword ***DEFINE_FUNCTION**.

Each damage parameter to determine the damage initiation and progression is accumulated in accordance with the quation (6), (9), and (10). The exponential parameters denoted as β and m in the equation (6) and (10), which correspond to the parameter DMGEXP and FADEXP in the keyword deck, are utilized in order to fit the trend of the damage evolution curve. Fig. 8 (a) and (b) are comparison of the damage initiation and progression curve in each deformation mode according to the square root of thermodynamic force. The results show that the damage model can successfully reproduce the actual damage progression in both compression and shear model. Fig.9 shows the comparison of the stress-strain relation in the compression continuous stress test [10]. The simulation is in good agreement with the experiment. From these results, the proposed damage model and modelling method with **MAGD** can capture characteristic material and damage properties of RO-FRTP.

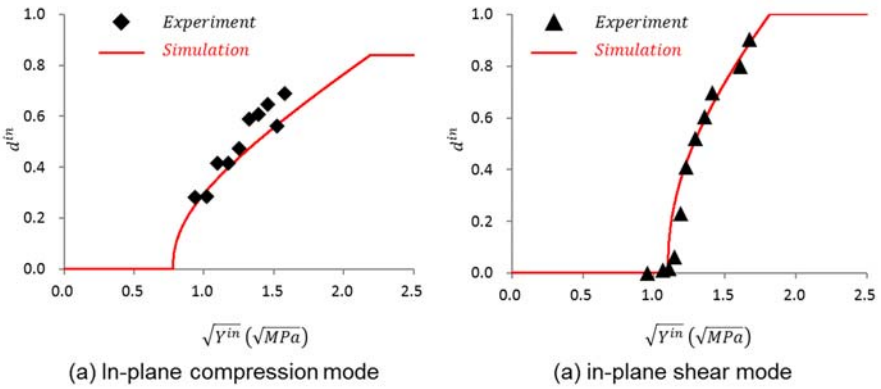

Fig.8: Compasison of the damage evolution according to the damage driving parameter in

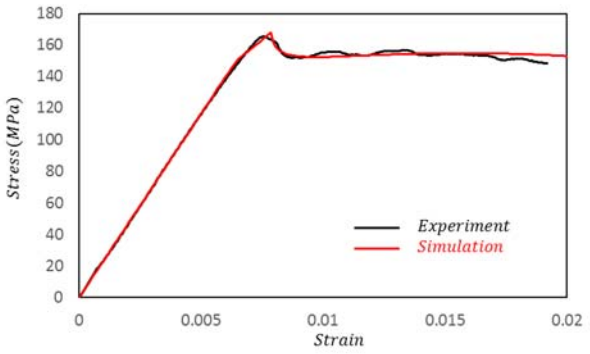

Fig.9: Comparison of stress and strain relation in compression continuous stress test.

Numerical simulation

Several numerical analyses were conducted with LS-DYNA® and compared to the experimental result in order to validate the proposed damage modelling method for RO-FRTP. For the validation, two kinds of three-point bending test, the flat plate and the closed hat shape, were simulated. In this study, 3D shell element of fully integrated shell formulation (ELFORM=16) was applied to the RO-FRTP sheet and the number of integration point in thickness direction was set to 9 (NIP=9).

5.1 Flat plate three-point bending analysis

The three-point bending analysis of flat plate was conducted and compared to the experimental result. Fig.10 shows FE model for the three-point bending test. Quasi-static load was applied to the punch which was modeled as rigid body. Contact conditions between the deformable flat plate and rigid bodies (punch, supports) were also defined. Fig.11(a) shows relation of reaction force and punch stroke. The simulation with LS-DYNA® is in good agreement with the experimental result and successfully captured the ductile behavior of RO-FRTP in the bending mode. Fig.11(b) shows longitudinal stress of integration points in the element near the punch. The number of each curve represents the location of the integration point through thickness direction. As the applied load increases, both tensile and compressive stress are also developed. While tensile stress keeps increasing, compressive stress becomes nearly constant after the stroke reaches 5mm in the lowest integration point and the constant stress distribution gradually spreads into thickness direction. This means that the compressive damage propagates as the applied load increases. The same damage propagation was also observed in the experiment [10].

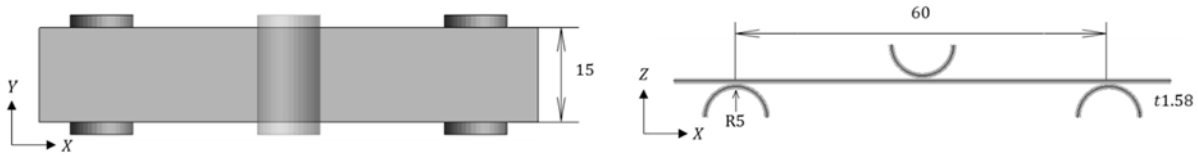

Fig.10: FE model for the three-point bending test of flat plate.

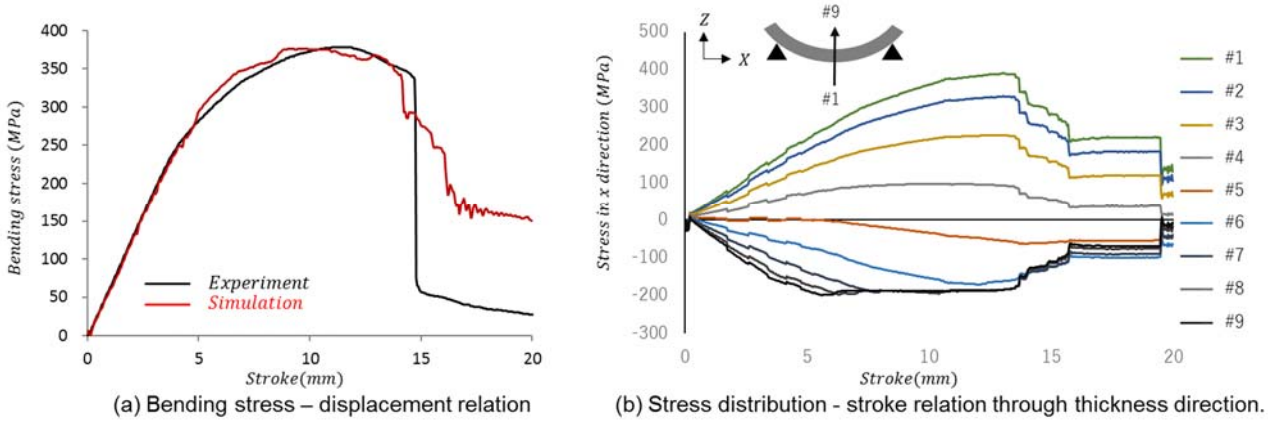

Fig.11: The result of the three-point bending simulation: (a) Force-displacement relation, (b) stress distribution through thickness.

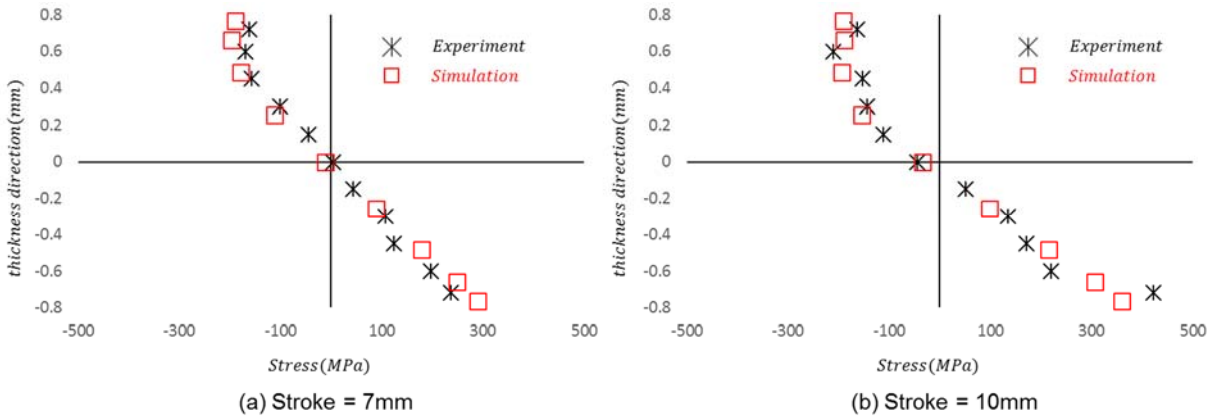

Fig.12: Comparison of stress distribution through thickness at the stroke of (a) 7mm and (b) 10mm.

Fig.12 shows the longitudinal stress distribution through thickness direction in the element near to the punch at the stroke of 7mm and 10mm. The stress values from the experiment were derived from strain measured by Digital Image Correlation analysis [10]. The result shows that the simulation also successfully captures the property under the bending deformation precisely.
These studies indicate that the proposed damage modelling has capability to reproduce the damage progression of RO-FRTP in detail and predict the bending deformation of the material accurately.

5.2 Three-point bending analysis of closed-hat-section beams

In order to evaluate the damage modelling for practical analyses, quasi-static and dynamic three-point bending analyses of closed-hat-section beam were conducted and compared to the experimental results. Fig.13 shows the FE model used for the analysis. The impactor and other supports were modeled as rigid bodies. In the dynamic simulation, mass of the impactor was adjusted to 118.7kg which is the same weight of the actual impactor. Initial velocity of the impactor was prescribed to be 30km/h which is also the same as that in the experiment. Fig.14 shows the comparison of reaction force – stroke relation of the impactor in the static and dynamic analysis. In the static load case, the reaction force is predicted with high accuracy throughout the whole analysis. The error of the predicted peak force and energy absorption (EA) are 3% or less. In the dynamic load case, the reaction force is also predicted well up to the peak. After the peak force, the load is gradually decreased in the same trend as the experiment. The error of the predicted peak force and EA are 9% or less. Fig.15 shows the deformation mode of each loading case and the in-plane damage distribution at the stroke of 36mm. The predicted deformation modes are in good agreement with those observed in the experiment.
These results suggest that the proposed damage modelling in this study is applicable to practical analyses conducted in the design process of RO-FRTP products.

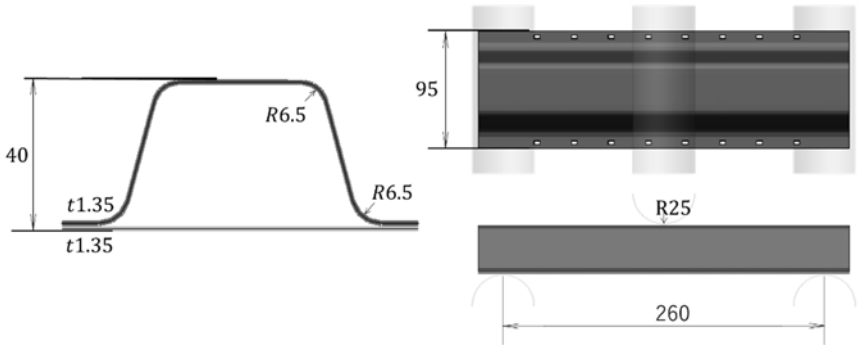

Fig.13: Configuration of hat shape for static and dynamic three-point bending analysis.

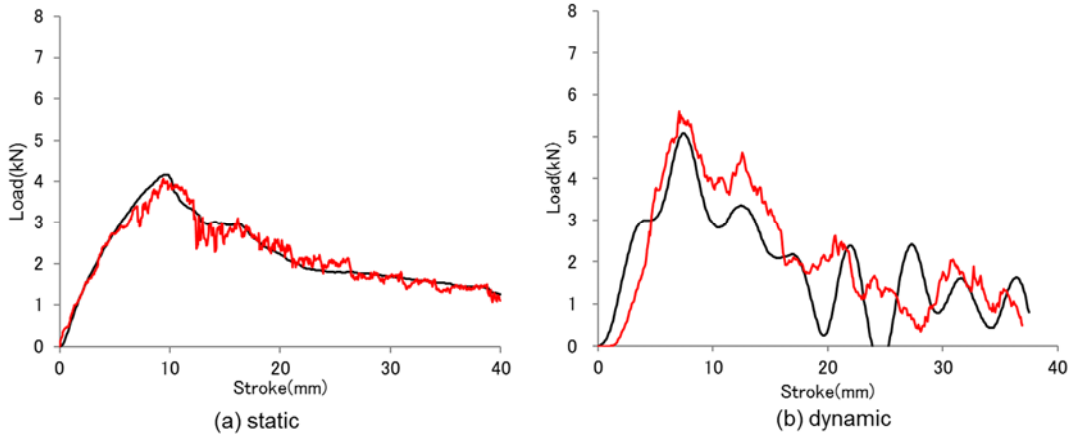

Fig.14: The comparison of reaction force and stroke of the impactor in (a) static and (b) dynamic three-point bending simulation of closed-hat-section beam.

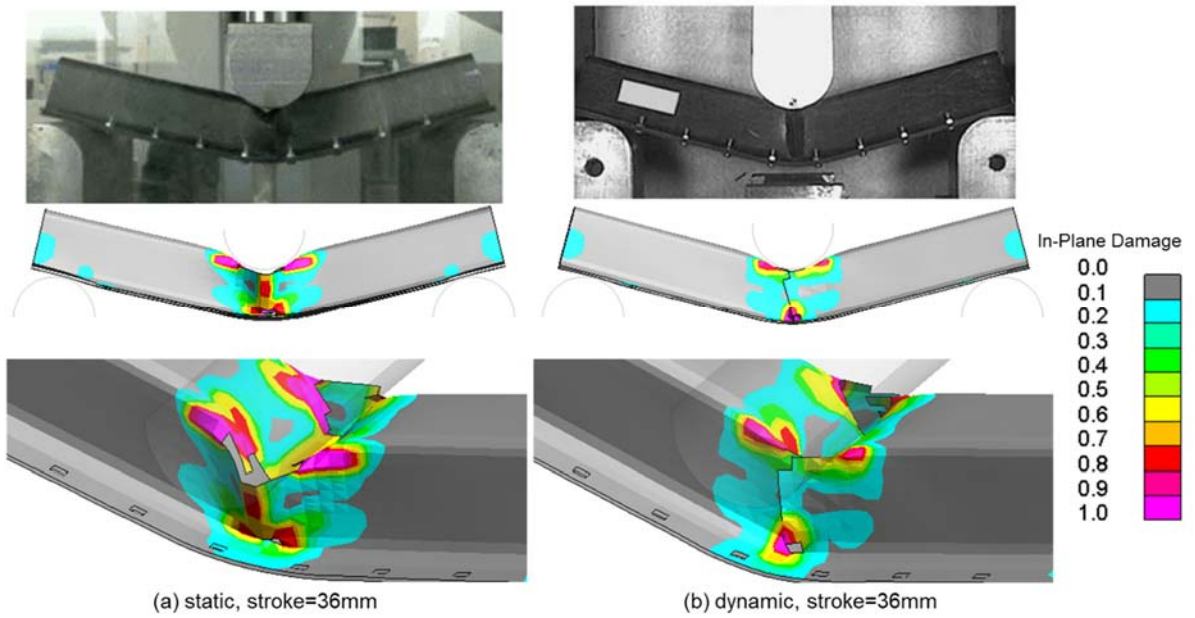

Fig.15: Comparison of deformation mode in static and dynamic three-point bending simulation of closed-hat-section beam.

6 Summary

In this study, the material and the damage modelling methods for RO-FRTP were proposed for 3D shell element. In order to reproduce the stress state dependent damage evolution with the single damage model, the highly functional damage modelling tool, **MAGD** in LS-DYNA®, was utilized. Furthermore, the user defined elastic plastic material model has been developed in order to transfer damage driving parameters that are necessary for the modelling. For the validation of the modelling method, several numerical studies have been conducted and compared to the experiments. The result suggests that the proposed method is able to model the damage characteristics of RO-FRTP accurately and applicable to the practical use of general analysis.

7 Literature

[1] Scott, P.: “The new BMW i3”, Retrieved April 6, 2019, from http://www.asymcar.com/graphics/14/i3/bmwi3b.pdf
[2] Sumiyama, T., Matsuo, T., Kan, M., Furuichi, K. et al.: “Non-Linear Finite Element Analysis for Three-Point Bending Behavior of Discontinuous and Randomly-Oriented Chopped Carbon Fiber Tape-Reinforced Thermoplastic”, Journal of the Japan Society for Composite Materials, 43(4),149-159, 2017.
[3] Erhart, T., Du Bois, P., Andrade, F.: “Short Introduction of a New Generalized Damage Model”, 11th European LS-DYNA Conference, 2017.
[4] Hallquist, J.O.: “LS-DYNA® Keyword User’s Manual, Volume II – Material Models”, LS-DYNA® R9.0, LSTC, 2016.
[5] Andrade, F. X. C., Feucht, M., Haufe, A., & Neukamm, F.: “An incremental stress state dependent damage model for ductile failure prediction”, International Journal of Fracture, 200(1-2), 2016, 127-150.
[6] JIS K 7164: “Plastics – Determination of tensile Properties – Part 4: Test Conditions for Isotropic and Orthotropic Fiber-Reinforced Plastic Composites”, Japanese Industrial Standards, 2005.
[7] JIS K 7076: “Testing Methods for Compressive Properties of Carbon Fiber Reinforced Plastics”, Japanese Industrial Standards, 1991.
[8] JIS K 7074: “Testing Methods for Flexural Properties of Carbon Fiber Reinforced Plastics”, Japanese Industrial Standards, 1988.
[9] JIS K 7079: “Testing Methods for In-Plane Shear Properties of Carbon Fiber Reinforced Plastics by $\pm 45°$ Tension Method and Two Pairs of Rails Method”, Japanese Industrial Standards, 1991.

[10] Hayashi, S., Kan, M., Saito, K., Nishi, M.: “Material and Damage Models of Randomly-Oriented Thermoplastic Composites for Crash Simulation”, SAE Technical Paper 2019-01-0814, 2019.
[11] Matsuo, T., Murakami, T., Kan, M., Sumiyama, T., et al.: “New Test Method for Nonlinear Out-of-Plane Shear Property Discontinuous and Randomly-Oriented Thermoplastic CFRP”, in the proceeding of the Symposium on Composite Materials, Kanazawa, 2015.